Chemical Science

ROYAL SOCIETY OF CHEMISTRY

EDGE ARTICLE

View Article Online
View Journal | View Issue

Cite this: *Chem. Sci.*, 2025, **16**, 20464

All publication charges for this article have been paid for by the Royal Society of Chemistry

Received 28th August 2025
Accepted 26th September 2025

DOI: 10.1039/d5sc06636k

rsc.li/chemical-science

Supercycloalkanes: dihydropyrazine-embedded macrocycles with flexible conformations resembling cycloalkanes

Shuhai Qiu,†[a] Li Zhang,†[a] Da-Hui Qu *[a] and Zhaohui Wang *[ab]

Cycloalkanoid molecules are of fundamental interest due to their unique geometric structures and physical properties. However, studies on the molecular dynamics of these molecules tend to be difficult owing to labile conformations. Herein, we report a series of "supercycloalkanes", namely dihydropyrazine-embedded macrocycles, that show puckered structures imitating those of cyclobutane, cyclopentane and cyclohexane, as confirmed by crystal structures. ^{1}H NMR spectrum analyses and theoretical calculations reveal that the macrocycle containing four dihydropyrazine corners undergoes a ring-flapping process in solution, and the one with five dihydropyrazine corners involves a pseudorotation process. Photophysical results indicate that these macrocycles show donor (D)–acceptor (A)-type structures, resulting in solvent-dependent emissions. Moreover, each dihydropyrazine corner could effectively interact with fullerene molecules owing to the V-shaped π-surface. This study provides a series of cycloalkanoids with a "superstructure" and discloses the molecular dynamics of cycloalkanoid macrocycles.

Introduction

Supermolecules, or superstructures, generally containing a series of periodic units with atomically precise structures, have aroused intense research interest due to their unique molecular structures and electronic properties.[1,2] These periodic units can be viewed as "superatoms", which dominantly describe nanoscale molecular clusters composed of inorganic cores and ligand shells in materials science.[3,4] However, studies on congeners with a pure covalent molecular skeleton are still limited. Some of the few examples include "superbenzenes" and "supernaphthalenes" (Fig. 1a), in which the carbon–carbon (C–C) bonds are expanded by replacement with π-spacers.[5–8] The supermolecules with well-defined molecular structures not only display inherent properties, such as aromaticity, of benzene or naphthalene, but also give rise to other unique features beyond, including red-shifted absorptions/emissions, redox properties, open-shell characteristics and so on.[7–9] More importantly, covalent "superstructures" even of nanometer size can be obtained *via* solution-phase synthesis. For example, Isobe and coworkers have reported the synthesis of atomically precise cylindrical phenine nanotubes with periodic vacancy defects, in which hollowed [6]cyclo-*meta*-phenylenes act as "superatoms" to replace the classic benzene units in carbon nanotubes.[10] These nanometer-sized molecules exhibited good solubility to allow for solution-phase analysis of their molecular structures, which is usually difficult for traditional carbon nanotubes. In spite of these impressive pioneering studies on covalent supermolecules, there is a lot of space to explore the chemistry and properties of other molecular systems.

Cycloalkanes, which contain a cyclic pure carbon skeleton, have been well studied by chemists in the early stages.[11] One of the hottest topics around these molecules focuses on molecular conformations and dynamics.[12,13] Due to the ideal angle of 109.5° among sp^3-hybridized carbon atoms, cycloalkanes tend to adopt puckered geometries to alleviate strain. Specifically, cyclobutane and cyclohexane have the lowest energy conformer with a folded and chair geometry, respectively, while cyclopentane has two types of conformers with nearly equal energy, the C_s symmetric envelope conformation with four carbon atoms in a plane and the C_2 symmetric half-chair form with three carbon atoms in a plane.[14,15] Theoretical calculations and infrared spectroscopic measurements revealed that cyclobutane underwent an inversion process with an energy barrier of less than 1.5 kcal mol^{-1} (Fig. 1b),[16–19] while cyclopentane underwent a pseudorotation process between the envelope and half-chair conformers (Fig. 1c).[20–22] However, the labile conformations of cyclobutane and cyclopentane preclude in-depth experimental studies, and only cyclohexane and higher cycloalkanes could be

[a]*Laboratory for Advanced Materials and Joint International Research Laboratory of Precision Chemistry and Molecular Engineering, Feringa Nobel Prize Scientist Joint Research Center, Frontiers Science Center for Materiobiology and Dynamic Chemistry, Institute of Fine Chemicals, School of Chemistry and Molecular Engineering, East China University of Science and Technology, Shanghai, 200237, P. R. China. E-mail: dahui_qu@ecust.edu.cn; wangzhaohui@mail.tsinghua.edu.cn*

[b]*Key Laboratory of Organic Optoelectronics and Molecular Engineering, Department of Chemistry, Tsinghua University, Beijing 100084, P. R. China*

† These authors contributed equally to this work.

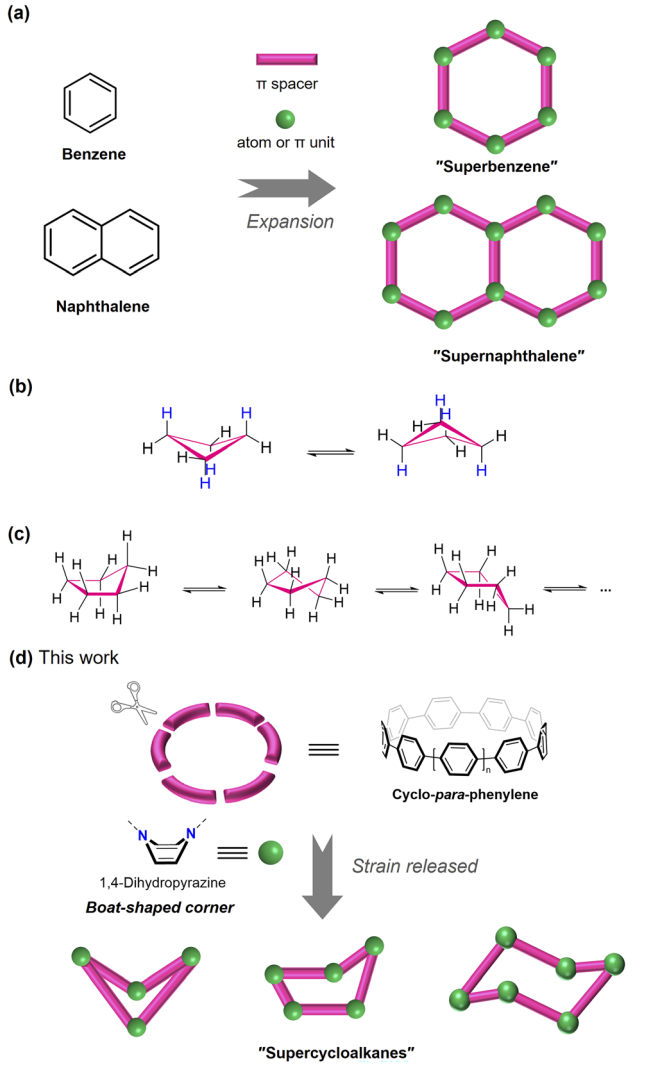

Fig. 1 (a) Representative examples of molecular designs towards superbenzenes and supernaphthalenes. (b) The inversion process of cyclobutane. (c) The pseudorotation process of cyclopentane. (d) Conceptual illustrations of molecular designs of supercycloalkanes in this work.

directly investigated using nuclear magnetic resonance (NMR) spectroscopy.[23,24] Therefore, cyclic molecules with sufficient conformational stability as well as similar molecular dynamics to cycloalkanes should be of interest. In the past decades, pioneering studies on cyclic oligomers constituted by *ortho*-linked aromatics, including benzene,[25,26] thiophene,[27] pyrene,[28] and porphyrins,[29] have been reported. Among them, most tetramers adopt a folded conformation in the solid state similar to that of cyclobutene, while higher aromatic oligomers, such as pentamers and hexamers, showing dynamic behaviors that resemble those of cyclopentane and cyclohexane, remain largely unexplored. Inspired by the less strained cycloalkanes, we envision that the installation of adaptive π-corners into the rigid skeleton of cyclo-*para*-phenylenes (CPPs)[30–33] should circumvent the high strain by regulating the corner angles and rotating around the diphenylene linkers; therefore, these polygonal macrocycles can act as "supercycloalkanes" that are structurally akin to cycloalkenes and display interesting molecular dynamics (Fig. 1d).

1,4-Dihydropyrazine is an 8π-electron antiaromatic ring,[34] and its π-extended derivatives, such as dihydrophenazines, have shown intriguing properties and functions, such as photoredox catalysis, tunable emissions, redox activity, and conformational dynamics.[35–38] On the one hand, by virtue of the antiaromatic character of dihydropyrazine, the hexagonal ring tends to adopt a V-shaped geometry in the ground state, especially when sterically hindered polycyclic aromatic units are fused.[39,40] On the other hand, the introduction of nitrogen atoms allows for the equatorial and axial exchanges on the substituents, providing more flexibility for conformational relaxation. Overall, these factors make dihydropyrazine derivatives ideal candidates as corners to construct π-conjugated polygonal macrocycles. Herein, we report the one-pot synthesis of dihydropyrazine-embedded macrocycles uniformly containing four to six dipyrene-fused dihydropyrazine corners, respectively. Instead of forming ideal polygonal tube-like structures, these macrocyclic molecules adopt puckered geometries as the lowest energy conformations similar to those of cycloalkanes, as unambiguously manifested by X-ray structures. The conformational analyses of these cyclic molecules are also studied using ^{1}H NMR spectra and theoretical calculations to obtain insight into the molecular dynamics of these flexible macrocycles. Moreover, these macrocycles exhibit intriguing properties, including D–A type electronic structures, and supramolecular interactions with fullerenes.

Results and discussion

Dihydropyrazine-embedded macrocycles were synthesized *via* a nickel-mediated Yamamoto coupling reaction of dipyreneo[*c*,*e*]dihydrophenazine dibromide **DPP-2Br**. During our exploration of axially N-embedded quasi-carbon nanohoops, this straightforward methodology successfully afforded the shape-persistent, cyclic dimer **DPP-D** and trimer **DPP-T** as the major products in yields of 20% and 45%, respectively, while trace amounts of higher oligomers up to the hexamer were detected by mass spectroscopy.[41] To ensure the favorable formation of higher oligomers, the reaction conditions, including the concentrations, temperature and solvents, were carefully controlled (Table S1). Finally, when the reaction was performed at high concentration (*ca.* 45 mM) in 2-methyltetrahydrofuran at 80 °C, the cyclic tetramer **DPP-Q**, pentamer **DPP-P** and hexamer **DPP-H** were isolated in yields of 8%, 5% and 1%, respectively, by using flash column chromatography or gel-permeable chromatography (GPC) (Scheme 1, see details in the SI). The molecular structures of **DPP-Q**, **DPP-P** and **DPP-H** were unambiguously confirmed by X-ray structures and spectroscopy measurements (*vide infra*). High-resolution mass spectra indicate a molecular weight of 3219.846 for **DPP-Q**, 4025.921 for **DPP-P**, and 4830.549 for **DPP-H** (Fig. S20–S22), respectively, with the isotopic pattern matching well with their corresponding molecular formula.

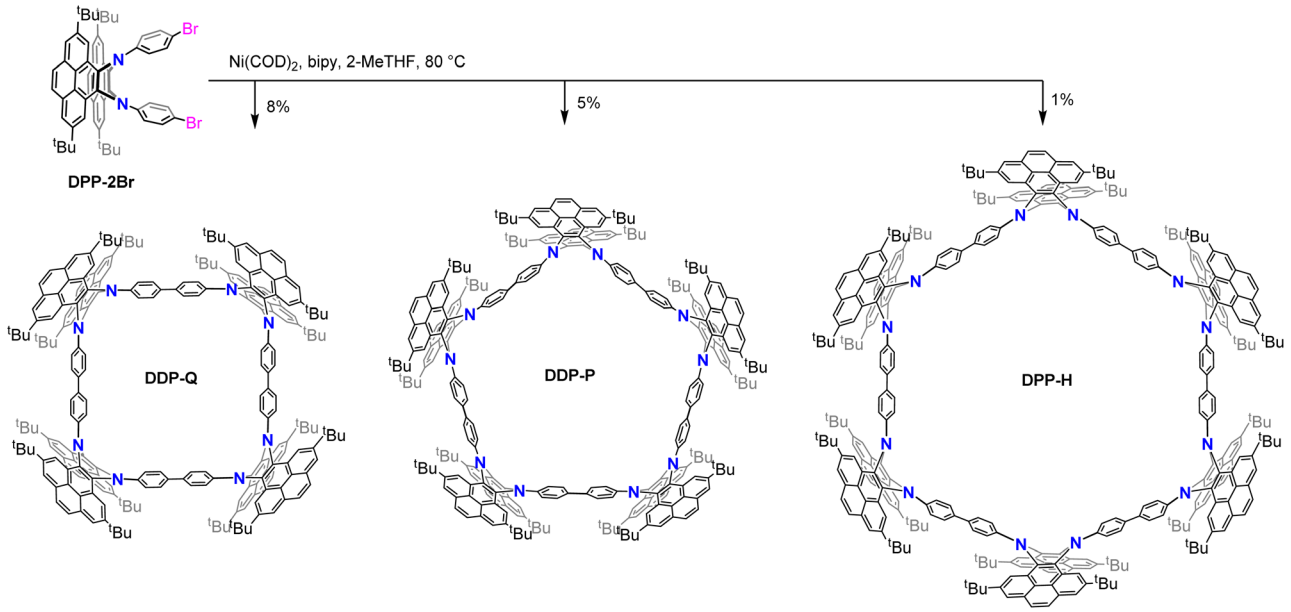

Scheme 1 Synthesis of macrocyclic oligomers **DPP-Q**, **DPP-P** and **DPP-H**.

Single crystals suitable for X-ray diffraction analyses were grown through slow evaporation of methanol into a chloroform solution for **DPP-Q** and **DPP-H** and a mesitylene solution for **DPP-P**. As shown in Fig. 2a, **DPP-Q** showed a puckered geometry with C_2 symmetry, slightly deviating from the ideal D_{2d} symmetric geometry for cyclobutane. The edge length of the folded structure, that is the diphenyl diamine linker, is around 10.0 Å. The distances between two centroids of the diagonal 1,4-dihydropyrazine rings are 12.7 and 14.9 Å, respectively. Correspondingly, the bending angles are measured to be 75.0° and 86.4°. Such a folded geometry could efficiently alleviate the strain, which is in line with the calculated strain energy of 6.1 kcal mol^{-1} according to hypothetical homodesmotic reactions (Scheme S1). This value is significantly lower than that of [12]

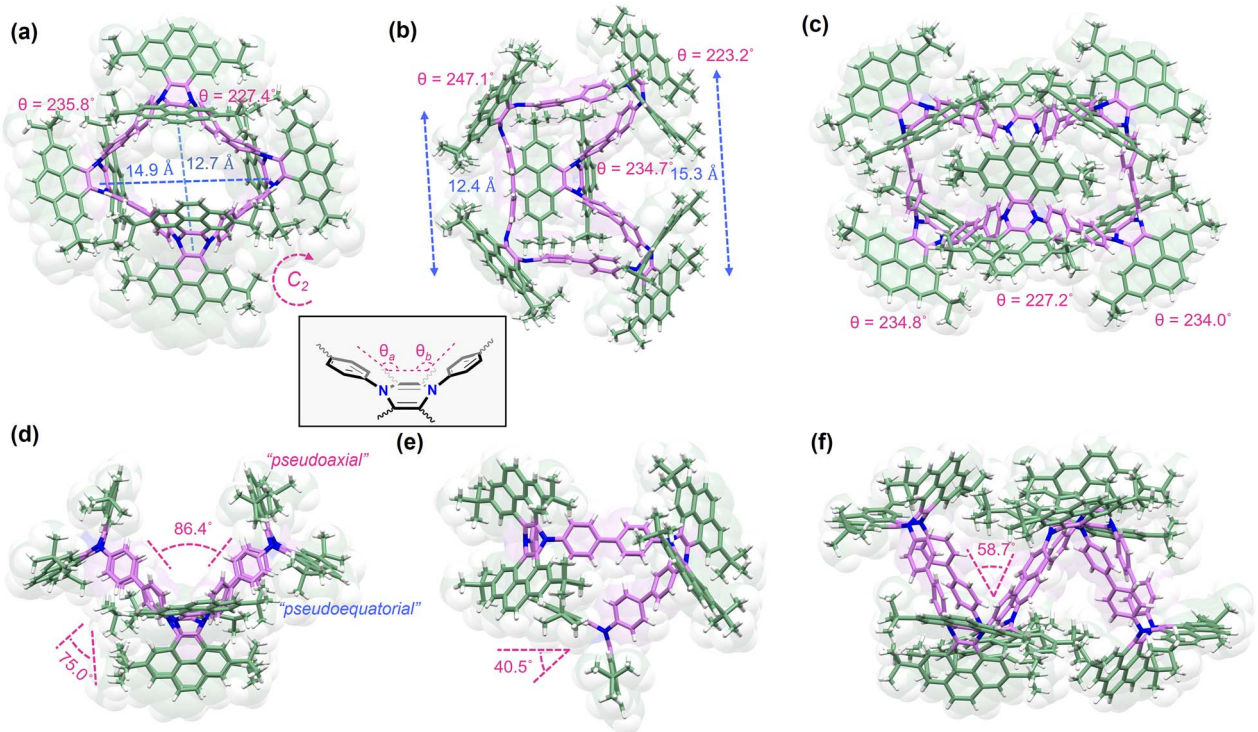

Fig. 2 X-ray crystallographic structures of **DPP-Q** (a: top view and d: side view), **DPP-P** (b: top view and e: side view), and **DPP-H** (c: top view and f: side view). Inset is an illustration of the bending angle in the dihydropyrazine corner.

CPP (48.1 kcal mol^{-1}),[42,43] indicating the high conformational flexibility of 1,2-dihydropyrazine corners. Interestingly, similar to sp^3-hybridized carbon atoms in cyclobutene, each dipyreneo [*c*,*e*]dihydrophenazine corner of **DPP-Q** has one pyrene unit at the pseudoequatorial position and the other one at the pseudoaxial position (Fig. 2d). Similarly, **DPP-P** and **DPP-H** also adopted puckered configurations to minimize the strain energy in the crystalline state. Specifically, only the C_s symmetric envelope configuration was observed for **DPP-P**, even though the C_2 symmetric half-chair conformation was reported to have a low energy close to that of the envelope form in the case of cyclopentane.[15] **DPP-H** adopted a chair-shaped geometry, in line with the lowest-energy conformation of cyclohexane.[44,45] The bending angle was measured to be 40.5°for **DPP-P** and 58.7° for **DPP-H**, respectively. Correspondingly, the strain energy was calculated to be 8.6 kcal mol^{-1} for **DPP-P** and 2.3 kcal mol^{-1} for **DPP-H**. Notably, the strain energy is closely correlated with the angle at each dihydropyrazine corner (θ), which can be defined as the sum of the angles between the N–N axis and phenyl groups at the N atoms (θ_a and θ_b, Fig. 2). The corner angles θ of both **DPP-Q** and **DPP-H** are in the range of 227.2–235.8°, which are slightly larger than that of the strainless precursor **DPP-2Br** (226.5°).[41] This is in agreement with the small strain energy of **DPP-Q** and **DPP-H**. However, in **DPP-P**, both the corner angles on the short edge (12.4 Å) of the trapezoid plane are 247.1°, much larger than that on the long edge side (θ = 223.2°). Such a large angle deviation from that of the strainless DPP unit leads to a higher strain than that of **DPP-Q** and **DPP-H**. As a result, the diphenyl linker in the short edge adopts a bent geometry, which is reminiscent of that of highly strained [*n*]CPPs.[30]

The molecular structures of **DPP-Q**, **DPP-P** and **DPP-H** in solution were investigated by variable-temperature (VT) ^{1}H NMR measurements. Considering the folded structure of **DPP-Q** in the crystalline state, two sets of ^{1}H NMR signals deriving from the pyrene units in both the pseudoequatorial and pseudoaxial positions were expected to appear. Interestingly, only one set of proton signals (δ = 8.06, 8.20 and 8.67 ppm) belonging to the pyrene unit of **DPP-Q** was observed in the aromatic region at 283 K (Fig. 3a), indicating that the protons of pyrene subunits at the pseudoequatorial positions are equal to those at the pseudoaxial positions. These results imply that the folded conformers probably undergo a fast inversion process to afford a time-average D_{4h} symmetric structure. As the temperature decreased from 283 K to 188 K, the signals gradually broadened due to a slowdown of conformational motions. When the temperature was lowered to the instrumental temperature limit of 173 K, each singlet signal belonging to the protons of pyrene subunits fully divided into two sets of peaks, suggesting that the inversion process is completely restricted, and the molecular structure adopts a folded D_{2d} symmetric geometry, in which the protons belonging to the pyrenes at the pseudoequatorial positions differ from those at the pseudoaxial positions. Based on line-shape analysis of proton signals, the exchange rate constant k at different temperatures was estimated according to the reported method developed by Gasparro and Kolodny[46] (see details in the SI). By fitting the parameter ln(k/T) *versus* the reciprocal number of temperature (1/T) to the Eyring equation (Fig. 3a, inset), the thermodynamic parameters $\Delta H^* = 8.33$ kcal mol^{-1} and $\Delta S^* = -2.54$ kcal mol^{-1} K^{-1} were obtained. Accordingly, the inversion energy barrier (ΔG^*) at the coalescence temperature (188 K) was determined to be 8.81 kcal mol^{-1}. This value matches well with theoretical calculations, which indicated that the inversion of the folded conformers overcame an energy barrier of 9.2 kcal mol^{-1} *via* a coplanar D_{4h} symmetric structure in the transition state (Fig. 3c). It is worth noting that this energy barrier is significantly higher than that of cyclobutane (1.45 kcal mol^{-1}),[19] which involves a rapid inversion process beyond the measurable range by NMR. Similar to **DPP-Q**, **DPP-P** also exhibited one set of proton signals belonging to the pyrene subunits (Fig. 3b), suggesting fast interconversion amongst all the conformers at room temperature. Further lowering the measurement temperature led to broadening of the proton signals, indicating the increased restrictions of conformational changes. Unfortunately, the conformational interconversion still occurred even at the temperature limit (173 K) as no signal split was observed. These results suggest that the conformational interconversion process of **DPP-P** has a relatively low energy barrier, lower than 5 kcal mol^{-1}, which is also reminiscent of the pseudorotation process of cyclopentane. In contrast to the inversion process with a high energy barrier of 5 kcal mol^{-1},[47] pseudorotation of cyclopentane generally proceeds without passing through a significant energy barrier, and the energy difference between the half-chair and envelope conformations is quite small with the envelope form being more stable by 0.5 kcal mol^{-1}.[48] However, owing to the labile conformations, experimental investigations on the pseudorotation process are still difficult.

In order to further understand the conformational dynamics of **DPP-P**, the conformational interconversion process was investigated by theoretical calculations. First, a ring-flipping process similar to that of **DPP-Q** was proposed (Fig. 3d). The D_{5h} symmetric transition state structure was optimized by relaxed scan to confine the N–N axis of 1,4-dihydropyrazine rings in coplanar positions. However, the high energy barrier of 24.4 kcal mol^{-1}, which is inconsistent with the results obtained from VT ^{1}H NMR measurements, precluded this hypothesis. Therefore, we assumed that the conformational interconversion of **DPP-P** might undergo a pseudorotation process, similar to that of cyclopentane.[49] Optimization of the molecular structures of **DPP-P** indicates that the energy of the envelope configuration is slightly higher than that of the half-chair one by 0.4 kcal mol^{-1}, which is in line with the slight energy difference between the two conformers in the case of cyclopentane. These results indicate that, instead of the inversion among the envelope conformers, a pseudorotation process involving both envelope and half-chair conformers is more feasible for **DPP-P**. In the case of **DPP-H**, multiple signals in ^{1}H NMR spectra were observed at room temperature (see Fig. S18), implying a high energy barrier in the conformational interconversion process compared to **DPP-Q** and **DPP-P**. However, further investigations on the molecular dynamics were impeded due to poor solubility even at a high temperature up to 413 K (Fig. S19).

To capture the conformational motions of these molecules, X-ray snapshots of different conformations were obtained by

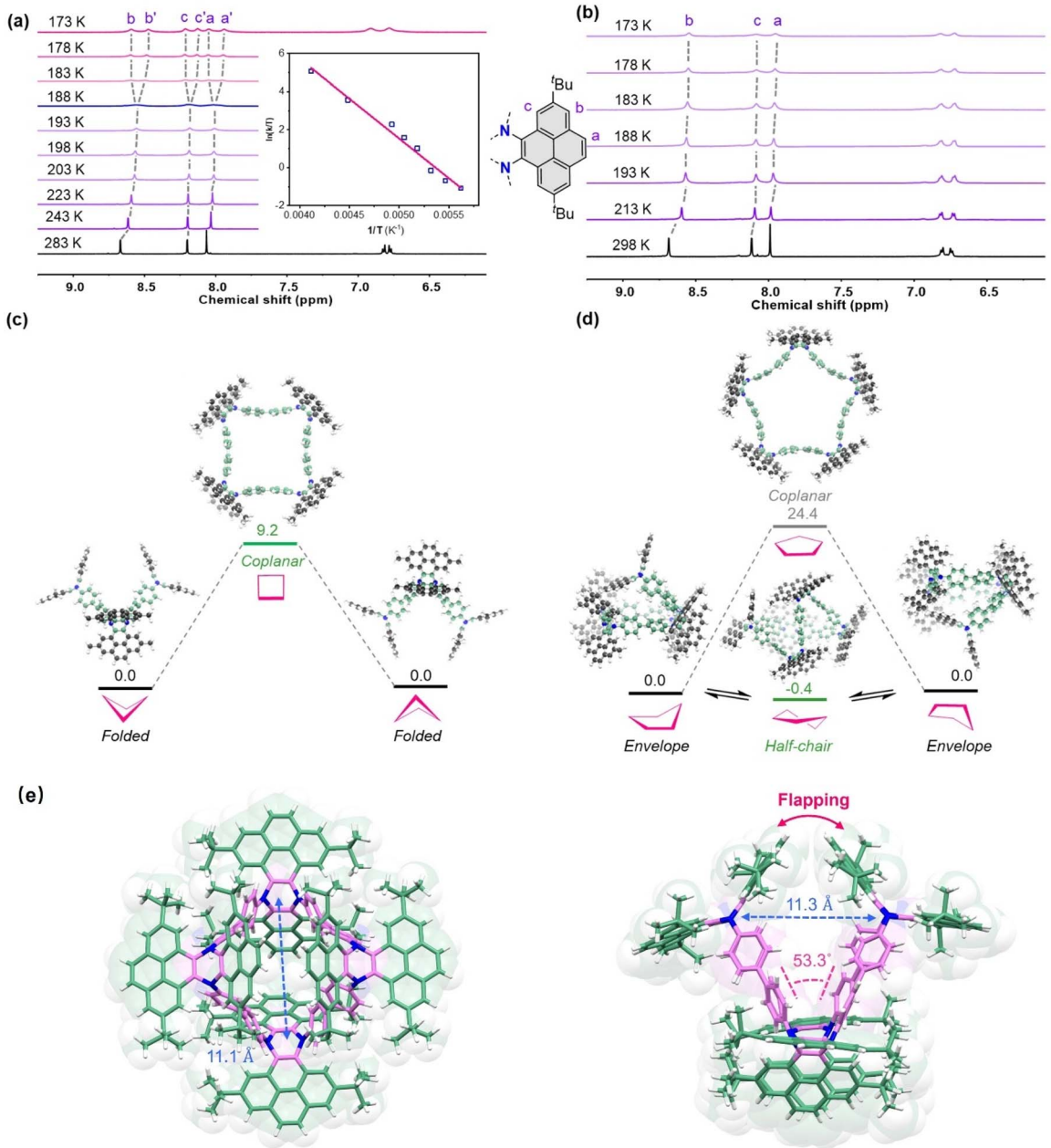

Fig. 3 Variable temperature ^{1}H NMR spectra (aromatic region, 600 M) of (a) **DPP-Q** and (b) **DPP-P** measured in dichloromethane-d_2. The proposed conformational dynamics of (c) **DPP-Q** and (d) **DPP-P** calculated at the B3LYP/6-31g(d) level. The inset shows plots and fits of the parameter ln(k/T) *versus* the reciprocal number of temperature (1/T). (e) X-ray snapshots of **DPP-Q** with a tightened geometry. Top view (left) and side view (right) are shown.

growing single crystals under various conditions. Single crystals of **DPP-Q** *via* slow evaporation of methanol into a 1,2-dichloroethane solution revealed a tightened conformation compared to that from the chloroform solution (Fig. 3e). The distances between two centroids of the diagonal 1,4-dihydropyrazine rings were shortened by 1.5–3.6 Å, and the bending angle was decreased by ~33°, which further supports a ring-flipping process as proposed in Fig. 3c.

The optical properties of these macrocyclic molecules were explored in solution (Fig. 4). Three molecules exhibited nearly identical absorptions in dichloromethane with the absorbance maximum at ~387 nm, which is also commonly observed in [n]CPPs.[50] All compounds exhibited green emission at different wavelengths (**DPP-Q:** 472 nm, **DPP-P:** 487 nm, and **DPP-H:** 476 nm), and the fluorescence quantum yields were measured to be 5.8% for **DPP-Q**, 6.8% for **DPP-P** and 5.3% for **DPP-H**. The fluorescence decay time determined using the nanosecond time-correlated single photon counting technique revealed a short lifetime of 2.0 ns for these molecules in dichloromethane (Fig. S7). The weak fluorescence and short emission lifetimes could be attributed to the fast conformational changes in solution. To further support this explanation,

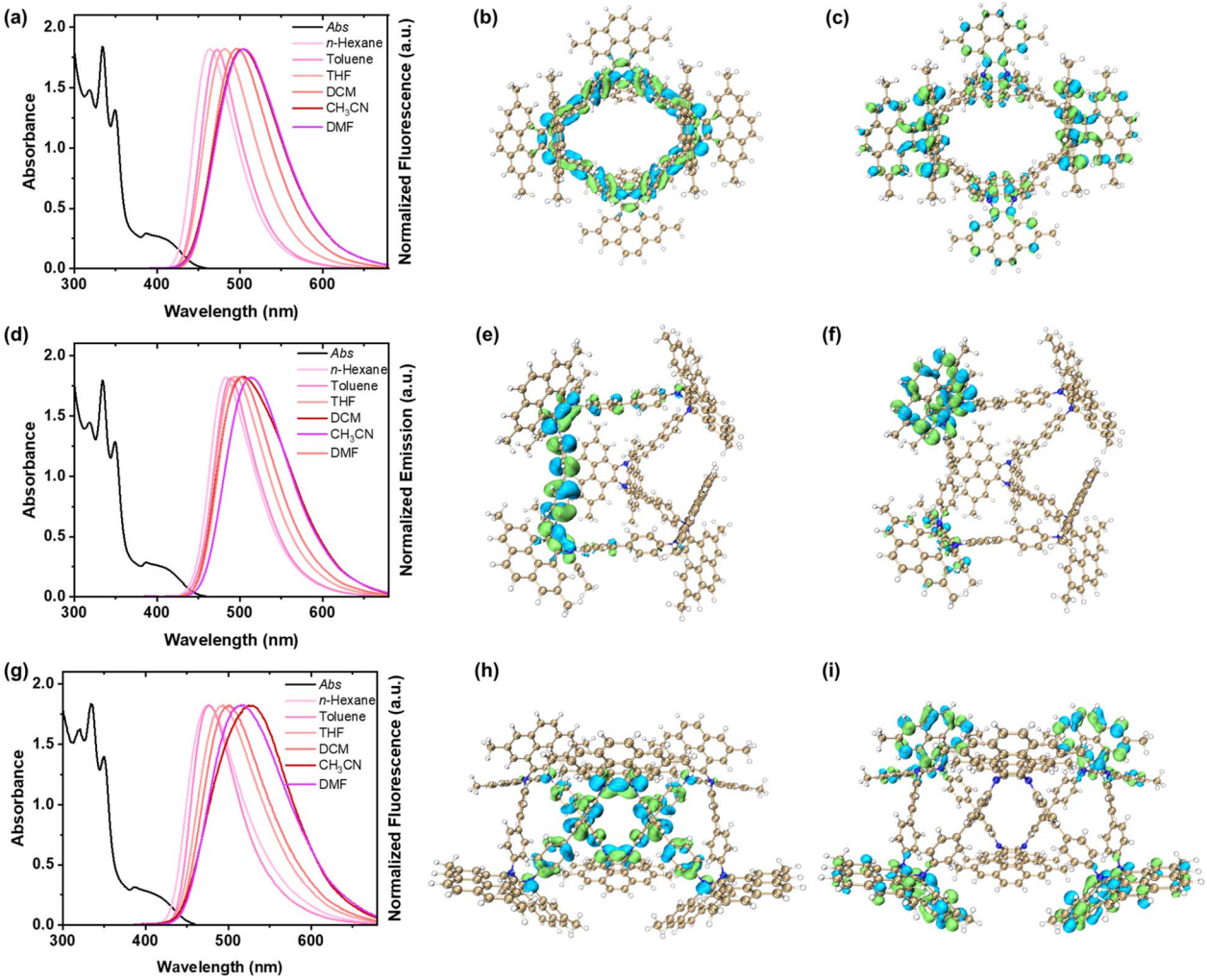

Fig. 4 Absorptions (in dichloromethane) and emissions of (a) **DPP-Q**, (d) **DPP-P** and (g) **DPP-H**. The concentration was 10 μM. Calculated frontier molecular orbitals of **DPP-Q** (b: HOMO and c: LUMO), **DPP-P** (e: HOMO and f: LUMO) and **DPP-H** (h: HOMO and i: LUMO).

variable temperature fluorescence of **DPP-Q** and **DPP-P** in toluene was measured by gradually lowering the temperature from room temperature to 78 K (Fig. S10). As the temperature was lowered to 113 K, only a small blue-shift in the emission (~5 nm for **DPP-Q** and ~10 nm for **DPP-P**) as well as limited enhancement of intensity was observed, which could be explained by the restrictions on the conformational inversions of the puckered structures, as supported by VT ^{1}H NMR results. When the temperature was further decreased to 78 K, the emission intensity dramatically increased, and a distinct blue-shift (~25 nm for **DPP-Q** and ~17 nm for **DPP-P**) was observed. These phenomena indicated a complete suppression of the conformation vibration of the DPP unit. These results also are consistent with reported π-extended dihydrophenazines, which involved bent-to-planar excited-state dynamics upon photoexcitation.[37,51]

The optical properties of these macrocycles in different solvents were also investigated. By modulating the polarity of the solvent, the absorptions showed negligible changes (Fig. S8). In contrast, the emission was distinctly red-shifted by 40 nm for **DPP-Q**, 30 nm for **DPP-P** and 52 nm for **DPP-H** (Fig. S9), which suggests that an intramolecular charge transfer process occurs upon excitation. These results are further supported by the disjoint distributions of the calculated frontier molecular orbitals (Fig. 4b–c, e, f, h and i). The highest occupied molecular orbitals (HOMOs) of **DPP-Q** localize on the whole dihydropyrazine-embedded CPP subunit, while the lowest unoccupied molecular orbitals (LUMOs) distribute on the pyrene units. In comparison to **DPP-Q**, the HOMOs of **DPP-P** and **DPP-H** distribute partially on the N-doped CPP skeleton, and the LUMOs localize on the partial pyrene units.

Considering the large cavity as well as the electron-rich structure, host–guest interactions of these macrocycles with fullerenes (C_{60} and C_{70}) were studied in solution. Fluorescence titration was performed by gradually adding fullerene molecules into a solution of **DPP-Q** or **DPP-P** in toluene (Fig. S11–S12). Fittings by monitoring the fluorescence changes (Fig. 5a–d) suggested a 1 : 1 binding mode for **DPP-Q** and **DPP-P**.[52] The association constant (K_a) of **DPP-Q** with C_{60} was determined to be 2.50×10^4 M^{-1}, while the K_a value with C_{70} was significantly higher at 1.86×10^5 M^{-1} in comparison with that with C_{60}. These results indicated a selective complexation of C_{70} over C_{60}

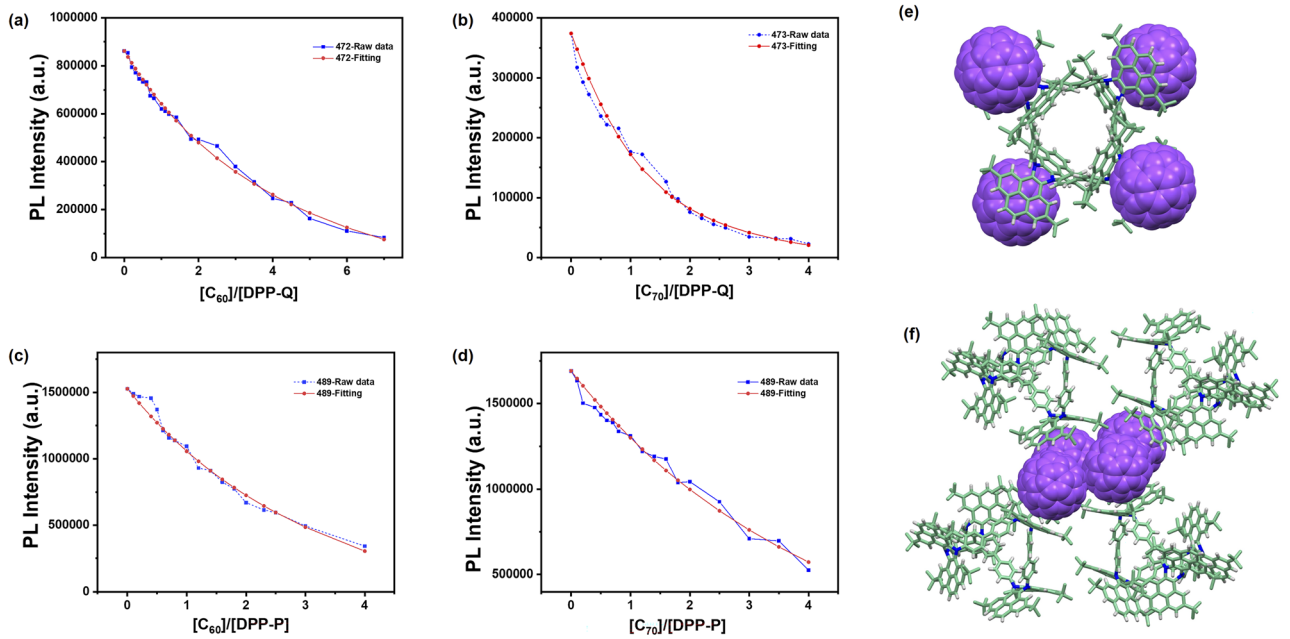

Fig. 5 Titration plots (blue) and fittings (red) of (a and b) **DPP-Q** and (c and d) **DPP-P** with different ratios of C_{60} or C_{70} measured in toluene at room temperature. The concentration of macrocycles was 10 μM. (e) Crystal structure and (f) assembly of **DPP-Q** and C_{60} molecules.

for **DPP-Q**. In contrast, **DPP-P** exhibited comparable K_a values of 3.13×10^4 M^{-1} with C_{60} and 2.02×10^4 M^{-1} with C_{70}, respectively, suggesting a similar binding affinity toward C_{60} and C_{70}.

In order to clarify the origins of supramolecular interactions with fullerenes, single crystals of the complexes were grown. Fortunately, single crystals of the complex **DPP-Q**@C_{60} suitable for X-ray analysis were obtained by slow evaporation of methanol into the **DPP-Q**/C_{60} mixture in toluene. As shown in Fig. 5e, one C_{60} molecule was located at the outside of each corner of **DPP-Q** with the distances of 3.22–3.35 Å, indicating strong interactions between the V-shaped π-surface and the convex of fullerenes. Notably, no C_{60} molecules were encapsulated in the cavity of **DPP-Q**, which might be attributed to the hindrance from the pyrene units at the openings. Therefore, the recognition selectivity of C_{70} over C_{60} can be explained by the larger π-surface of C_{70} molecules. Moreover, four C_{60} molecules aggregated together among **DPP-Q** molecules, forming a highly ordered supramolecular assembly (Fig. 5f and S13). In the case of **DPP-P**, the overcrowded configuration as well as the rapid conformational changes might restrict the interactions with fullerenes, thus affording moderate K_a values. It is worth noting that electron donor–acceptor systems have been proved to be essential for applications including photovoltaics and molecular electronics;[53,54] thus, these complexes of the electron-rich macrocycles with fullerenes might hold potential for applications in materials science in the future.

Conclusions

In summary, a series of "supercycloalkanes", namely dihydropyrazine-embedded macrocycles containing four to six dihydropyrazine corners, were synthesized and characterized. X-ray structures revealed that these macrocycles exhibited puckered geometries, which are reminiscent of the lowest energy conformations of cycloalkanes. ^{1}H NMR measurements, together with theoretical calculations, suggest that the macrocycle with four corners undergoes a ring-flapping process with an inversion barrier of *ca.* 9 kcal mol^{-1}, while the one containing five corners undergoes a pseudorotation process, which are in line with the conformational dynamics of cyclobutane and cyclopentane. Additionally, these "supercycloalkanes" exhibit unique properties, including D–A type electronic structures, and supramolecular interactions with fullerenes, which are absent for cycloalkanes. Our study not only presents a series of new cycloalkanoids with a "superstructure" that helps to understand their molecular dynamics, but also possesses potential for applications in materials science.

Author contributions

Z. W. and D.-H. Q. conducted the project administration and validation and acquired the financial support. S. Q. and L. Z. performed the research investigation and performed the synthesis, characterization, data analysis and draft writing. D.-H. Q. and Z. W. were responsible for the verification of data and completion of the whole manuscript. All authors have given approval to the final version of the manuscript.

Conflicts of interest

There are no conflicts to declare.

Data availability

CCDC 2417888–2417891 and 2479062 contain the supplementary crystallographic data for this paper.[55a–e]

The data supporting this article have been included as part of the SI. Supplementary information: synthetic details, spectroscopic measurements and theoretical calculations. See DOI: https://doi.org/10.1039/d5sc06636k.

Acknowledgements

This work was supported by the National Natural Science Foundation of China (Grants 22235005 and 22461160284), the Innovation Program of the Shanghai Municipal Education Commission (Grant 2023ZKZD40). The authors thank the Feringa Nobel Prize Scientist Joint Research Center and Research Center of the Analysis and Test of East China University of Science and Technology for help with the material characterization.

Notes and references

1 J.-M. Lehn, Supramolecular Chemistry—Scope and Perspectives Molecules, Supermolecules, and Molecular Devices (Nobel Lecture), *Angew. Chem., Int. Ed.*, 1988, **27**, 89–112.
2 Y. Ortiz Acero, D. Bhatacharya, D. Klein and J. F. Liebman, Super-molecules, *Rev. Roum. Chim.*, 2016, **61**, 269–276.
3 E. A. Doud, A. Voevodin, T. J. Hochuli, A. M. Champsaur, C. Nuckolls and X. Roy, Superatoms in materials science, *Nat. Rev. Mater.*, 2020, **5**, 371–387.
4 A. Pinkard, A. M. Champsaur and X. Roy, Molecular Clusters: Nanoscale Building Blocks for Solid-State Materials, *Acc. Chem. Res.*, 2018, **51**, 919–929.
5 R. Chauvin and I. Carbomers, A general concept of expanded molecules, *Tetrahedron Lett.*, 1995, **36**, 397–400.
6 K. Cocq, C. Lepetit, V. Maraval and R. Chauvin, "Carbo-aromaticity" and novel carbo-aromatic compounds, *Chem. Soc. Rev.*, 2015, **44**, 6535–6559.
7 Z. Li, T. Y. Gopalakrishna, Y. Han, Y. Gu, L. Yuan, W. Zeng, D. Casanova and J. Wu, [6]Cyclo-para-phenylmethine: An Analog of Benzene Showing Global Aromaticity and Open-Shell Diradical Character, *J. Am. Chem. Soc.*, 2019, **141**, 16266–16270.
8 Y. Ma, Y. Han, X. Hou, S. Wu and C. Chi, Facile Synthesis and Global Aromaticity of Aza-Superbenzene and Aza-Supernaphthalene at Different Oxidation States, *Angew. Chem., Int. Ed.*, 2024, **63**, e202407990.
9 K. Cocq, V. Maraval, N. Saffon-Merceron, A. Saquet, C. Poidevin, C. Lepetit and R. Chauvin, Carbo-Quinoids: Stability and Reversible Redox-Proaromatic Character towards Carbo-Benzenes, *Angew. Chem., Int. Ed.*, 2015, **54**, 2703–2706.
10 Z. Sun, K. Ikemoto, T. M. Fukunaga, T. Koretsune, R. Arita, S. Sato and H. Isobe, Finite phenine nanotubes with periodic vacancy defects, *Science*, 2019, **363**, 151–155.
11 V. Dragojlovic, Conformational analysis of cycloalkanes, *ChemTexts*, 2015, **1**, 14.
12 M. A. Winnik, Cyclization and the conformation of hydrocarbon chains, *Chem. Rev.*, 1981, **81**, 491–524.
13 F. Anet, A. Cheng and J. Wagner, Determination of conformational energy barriers in medium-and large-ring cycloalkanes by proton and carbon-13 nuclear magnetic resonance, *J. Am. Chem. Soc.*, 1972, **94**, 9250–9252.
14 E. L. Eliel and S. H. Wilen, *Stereochemistry of organic compounds*, John Wiley & Sons, 1994.
15 J. E. Kilpatrick, K. S. Pitzer and R. Spitzer, The Thermodynamics and Molecular Structure of Cyclopentane, *J. Am. Chem. Soc.*, 1947, **69**, 2483–2488.
16 E. D. Glendening and A. M. Halpern, Ab initio study of cyclobutane: Molecular structure, ring-puckering potential, and origin of the inversion barrier, *J. Phys. Chem. A*, 2005, **109**, 635–642.
17 G. W. Rathjens Jr, N. K. Freeman, W. D. Gwinn and K. S. Pitzer, Infrared Absorption Spectra, Structure and Thermodynamic Properties of Cyclobutane1, *J. Am. Chem. Soc.*, 1953, **75**, 5634–5642.
18 T. Ueda and T. Shimanouchi, Dihedral Angle and Ring-Puckering Potential of Cyclobutane, *J. Chem. Phys.*, 1968, **49**, 470–471.
19 J. M. R. Stone and I. M. Mills, Puckering structure in the infra-red spectrum of cyclobutane, *Mol. Phys.*, 1970, **18**, 631–652.
20 J. P. McCullough, Pseudorotation in Cyclopentane and Related Molecules, *J. Chem. Phys.*, 1958, **29**, 966–967.
21 R. Poupko, Z. Luz and H. Zimmermann, Pseudorotation in cyclopentane. An experimental determination of the puckering amplitude by NMR in oriented solvents, *J. Am. Chem. Soc.*, 1982, **104**, 5307–5314.
22 L. E. Bauman and J. Laane, Pseudorotation of cyclopentane and its deuterated derivatives, *J. Phys. Chem.*, 1988, **92**, 1040–1051.
23 B. D. Ross and N. S. True, NMR spectroscopy of cyclohexane. Gas-phase conformational kinetics, *J. Am. Chem. Soc.*, 1983, **105**, 4871–4875.
24 K. B. Wiberg, J. D. Hammer, H. Castejon, W. F. Bailey, E. L. DeLeon and R. M. Jarret, Conformational Studies in the Cyclohexane Series. 1. Experimental and Computational Investigation of Methyl, Ethyl, Isopropyl, and tert-Butylcyclohexanes, *J. Org. Chem.*, 1999, **64**, 2085–2095.
25 H. Jiang, Y. Zhang, D. Chen, B. Zhou and Y. Zhang, An Approach to Tetraphenylenes via Pd-Catalyzed C–H Functionalization, *Org. Lett.*, 2016, **18**, 2032–2035.
26 I. L. Karle and L. O. Brockway, The Structures of Biphenyl, o-Terphenyl and Tetraphenylene1, *J. Am. Chem. Soc.*, 1944, **66**, 1974–1979.
27 M. Iyoda and H. Shimizu, Multifunctional π-expanded oligothiophene macrocycles, *Chem. Soc. Rev.*, 2015, **44**, 6411–6424.
28 D. Popp, S. M. Elbert, C. Barwig, J. Petry, F. Rominger and M. Mastalerz, Palladium-Catalyzed Cyclization of a Pyryne Precursor to Higher Pyrenylenes, *Angew. Chem., Int. Ed.*, 2023, **62**, e202219277.
29 H. He, S. Lee, N. Liu, X. Zhang, Y. Wang, V. M. Lynch, D. Kim, J. L. Sessler and X.-S. Ke, Cyclic Carbaporphyrin Arrays, *J. Am. Chem. Soc.*, 2023, **145**, 3047–3054.

30 M. R. Golder and R. Jasti, Syntheses of the Smallest Carbon Nanohoops and the Emergence of Unique Physical Phenomena, *Acc. Chem. Res.*, 2015, **48**, 557–566.
31 Y. Segawa, A. Yagi, K. Matsui and K. Itami, Design and Synthesis of Carbon Nanotube Segments, *Angew. Chem., Int. Ed.*, 2016, **55**, 5136–5158.
32 S. E. Lewis, Cycloparaphenylenes and related nanohoops, *Chem. Soc. Rev.*, 2015, **44**, 2221–2304.
33 M. Hermann, D. Wassy and B. Esser, Conjugated nanohoops incorporating donor, acceptor, hetero-or polycyclic aromatics, *Angew. Chem., Int. Ed.*, 2021, **60**, 15743–15766.
34 F. W. Fowler and S.-J. Chen, Synthesis of the 1,4-dihydropyrazine ring system. Stable 8.pi.-electron heterocycle, *J. Org. Chem.*, 1971, **36**, 4025–4028.
35 T. Okamoto, E. Terada, M. Kozaki, M. Uchida, S. Kikukawa and K. Okada, Facile synthesis of 5,10-diaryl-5,10-dihydrophenazines and application to EL devices, *Org. Lett.*, 2003, **5**, 373–376.
36 J. C. Theriot, C. H. Lim, H. Yang, M. D. Ryan, C. B. Musgrave and G. M. Miyake, Organocatalyzed atom transfer radical polymerization driven by visible light, *Science*, 2016, **352**, 1082–1086.
37 Z. Zhang, Y. S. Wu, K. C. Tang, C. L. Chen, J. W. Ho, J. Su, H. Tian and P. T. Chou, Excited-State Conformational/Electronic Responses of Saddle-Shaped N,N'-Disubstituted-Dihydrodibenzo[a,c]phenazines: Wide-Tuning Emission from Red to Deep Blue and White Light Combination, *J. Am. Chem. Soc.*, 2015, **137**, 8509–8520.
38 G. L. Dai, Y. He, Z. H. Niu, P. He, C. K. Zhang, Y. Zhao, X. H. Zhang and H. S. Zhou, A Dual- Ion Organic Symmetric Battery Constructed from PhenazineBased Artificial Bipolar Molecules, *Angew. Chem., Int. Ed.*, 2019, **58**, 9902–9906.
39 S. Qiu, Z. Zhang, Z. Wang, D.-H. Qu and H. Tian, Tailor-Made Dynamic Fluorophores: Precise Structures Controlling the Photophysical Properties, *Precis. Chem.*, 2023, **1**, 129–138.
40 Z. Y. Zhang, W. X. Song, J. H. Su and H. Tian, Vibration-Induced Emission (VIE) of N,N′-Disubstituted-Dihydribenzo[a,c]phenazines: Fundamental Understanding and Emerging Applications, *Adv. Funct. Mater.*, 2020, **30**, 1902803.
41 S. Qiu, Y. Zhao, L. Zhang, Y. Ni, Y. Wu, H. Cong, D.-H. Qu, W. Jiang, J. Wu, H. Tian and Z. Wang, Axially *N*-Embedded Quasi-Carbon Nanohoops with Multioxidation States, *CCS Chem.*, 2023, **5**, 1763–1772.
42 Y. Segawa, H. Omachi and K. Itami, Theoretical Studies on the Structures and Strain Energies of Cycloparaphenylenes, *Org. Lett.*, 2010, **12**, 2262–2265.
43 E. R. Darzi and R. Jasti, The dynamic, size-dependent properties of [5]–[12]cycloparaphenylenes, *Chem. Soc. Rev.*, 2015, **44**, 6401–6410.
44 D. A. Dixon and A. Komornicki, Ab initio conformational analysis of cyclohexane, *J. Phys. Chem.*, 1990, **94**, 5630–5636.
45 K. B. Wiberg, Conformational Studies in the Cyclohexane Series. 3. The Dihalocyclohexanes, *J. Org. Chem.*, 1999, **64**, 6387–6393.
46 F. P. Gasparro and N. H. Kolodny, NMR determination of the rotational barrier in N, N-dimethylacetamide. A physical chemistry experiment, *J. Chem. Edu.*, 1977, **54**, 258.
47 I. Kolossvary and W. C. Guida, Comprehensive conformational analysis of the four-to twelve-membered ring cycloalkanes: identification of the complete set of interconversion pathways on the MM2 potential energy hypersurface, *J. Am. Chem. Soc.*, 1993, **115**, 2107–2119.
48 K. S. Pitzer and W. E. Donath, Conformations and strain energy of cyclopentane and its derivatives, *J. Am. Chem. Soc.*, 1959, **81**, 3213–3218.
49 W. J. Adams, H. J. Geise and L. S. Bartell, Structure, equilibrium conformation, and pseudorotation in cyclopentane. An electron diffraction study, *J. Am. Chem. Soc.*, 1970, **92**, 5013–5019.
50 E. R. Darzi and R. Jasti, The dynamic, size-dependent properties of [5]-[12]cycloparaphenylenes, *Chem. Soc. Rev.*, 2015, **44**, 6401–6410.
51 S. Qiu, Z. Zhang, Y. Wu, F. Tong, K. Chen, G. Liu, L. Zhang, Z. Wang, D.-H. Qu and H. Tian, Vibratile Dihydrophenazines with Controllable Luminescence Enabled by Precise Regulation of π-Conjugated Wings, *CCS Chem.*, 2022, **4**, 2344–2353.
52 P. Thordarson, Determining association constants from titration experiments in supramolecular chemistry, *Chem. Soc. Rev.*, 2011, **40**, 1305–1323.
53 H. Hölzel, P. Haines, R. Kaur, D. Lungerich, N. Jux and D. M. Guldi, Probing Charge Management across the π-Systems of Nanographenes in Regioisomeric Electron Donor–Acceptor Architectures, *J. Am. Chem. Soc.*, 2022, **144**, 8977–8986.
54 J. Sukegawa, C. Schubert, X. Zhu, H. Tsuji, D. M. Guldi and E. Nakamura, Electron transfer through rigid organic molecular wires enhanced by electronic and electron–vibration coupling, *Nat. Chem.*, 2014, **6**, 899–905.
55 (*a*) S. Qiu, L. Zhang, D.-H. Qu and Z. Wang, CCDC 2417888: Experimental Crystal Structure Determination, 2025, DOI: **10.5517/ccdc.csd.cc2m50d7**; (*b*) S. Qiu, L. Zhang, D.-H. Qu and Z. Wang, CCDC 2417889: Experimental Crystal Structure Determination, 2025, DOI: **10.5517/ccdc.csd.cc2m50f8**; (*c*) S. Qiu, L. Zhang, D.-H. Qu and Z. Wang, CCDC 2417890: Experimental Crystal Structure Determination, 2025, DOI: **10.5517/ccdc.csd.cc2m50g9**; (*d*) S. Qiu, L. Zhang, D.-H. Qu and Z. Wang, CCDC 2417891: Experimental Crystal Structure Determination, 2025, DOI: **10.5517/ccdc.csd.cc2m50hb**; (*e*) S. Qiu, L. Zhang, D.-H. Qu and Z. Wang, CCDC 2479062: Experimental Crystal Structure Determination, 2025, DOI: **10.5517/ccdc.csd.cc2p6nrb**.